IEEE Access
Multidisciplinary | Rapid Review | Open Access Journal

Received January 14, 2020, accepted February 25, 2020, date of publication February 28, 2020, date of current version March 12, 2020.

Digital Object Identifier 10.1109/ACCESS.2020.2977135

Thermal Deformation Suppression Chip Based on Material Symmetry Design for Single Center Supported MEMS Devices

BOWEN XING[1], BIN ZHOU[1], XINXI ZHANG[2], WENMING ZHANG[1], BO HOU[1], QI WEI[1], TIAN ZHANG[3], AND RONG ZHANG[1]

[1]Precision Measurement Technology and Instruments, Tsinghua University, Beijing 100084, China
[2]Weapon and Control Department, Army Academy of Armored Forces, Beijing 100072, China
[3]Beijing Institute of Computer and Electronics Application, Beijing 100084, China

Corresponding author: Bowen Xing (xingbw17@mails.tsinghua.edu.cn)

This work was supported in part by the National Key Research and Development Program of China under Grant 2018YFB1702500, and in part by the National Natural Science Foundation of China under Grant 41871245.

ABSTRACT Structural thermal deformation is an important factor that affects the performance of MEMS devices. The mismatch of thermal expansion coefficient (CTE) between different materials is a major source. For single center supported MEMS devices, expansion difference between device and the substrate leads to the out of plane thermal deformation of the structure, resulting in the performance deterioration. This paper presents a thermal deformation suppression chip (TDSC) for single center supporting MEMS devices. It is fabricated by the MEMS process and consists of an upper plate and a lower plate. The materials of the upper and lower plates are the same as those of the device substrate and structure respectively. The principle of TDSC to suppress thermal deformation is material symmetry design. Single center anchor is adapted to connect the upper and lower plates. Besides, the center anchor can also isolate the packaging stress generated between TDSC and package shell. In this paper, center supported quadruple mass gyroscope (CSQMG) is used to verify the effect of TDSC. Finite element simulation shows that the thermal deformation suppression effect is determined by radius of TDSC anchor, and the deformation can be suppressed to 0. The conclusion is confirmed by White light interference experiment. In addition, the experiment results also show that the TDSC effectively reduce the thermal out-of-plane deformation after packaging, which is even better than that of the gyroscope without any packaging. It is further proved that TDSC can also significantly improve the temperature performance of the CSQMG. Moreover, the TDSC has simple process steps, small chip area, low cost, and is suitable for various MEMS devices with single center anchor.

INDEX TERMS CTE mismatch, single center supported, material symmetry, thermal deformation suppression chip, packaging stress isolation.

I. INTRODUCTION

MEMS (microelectromechanical system) is an interdisciplinary technology field, involving microelectronics, machinery, optics, biology, materials, physics, chemistry, signal processing, and other disciplines. Microsensors based on MEMS technology have the advantages of small size, low power consumption, and low cost. MEMS devices have a significant impact on consumption, industry, and other important fields. With the developments in technology, the requirement for the accuracy and environmental adaptability of MEMS devices has significantly increased [1], [2].

Mechanical deformation is an important factor affecting the performance of sensors. Some MEMS devices such as gyroscope [3], [4], pressure sensor [5], [6], and accelerometer [7] work on the principle of force conversion. In such cases, these sensors convert the external signals (acceleration, angular velocity, pressure) to electrical signals, and detect the electrical signals to achieve high-precision measurement. However, thermal deformation directly leads to output error [8]. In general, stress and thermal deformation occur together. Structural stress will cause stiffness asymmetry,

The associate editor coordinating the review of this manuscript and approving it for publication was Sanket Goel.

coupling modal motion, and frequency drift [9]. Some reports demonstrate that thermal stress can cause deformation or even fatigue fracture in the movable structure, which have the most direct impact on output, and the relationship between thermal deformation and temperature is normally nonlinear. Thus, the performance of the device will be worse under the condition of variable temperature [10]–[12]. Consequently, stress and thermal deformation minimization has become an important issue.

Generally, a main source of thermal deformation is the coefficient of thermal expansion (CTE) mismatch [13]–[15] For most solid materials, when the temperature of an object with a length L changes, the free thermal expanding is defined by

$$\frac{dL}{dT} = \alpha_T L \tag{1}$$

where α_T is the coefficient of thermal expansion (CTE) of the object and T_0 is the reference temperature. For some MEMS devices, the material of device is different from that of the substrate, which is determined by process method, such as hemispherical resonator gyro, device based on the silicon on glass (SOG). Besides, MEMS packaging is used to protect device structures and provide electrical interconnection. MEMS devices and matching circuit chips are encapsulated in a shell to form a micro-sensor, which can be used independently. It is really difficult to select the same material as the device to complete packaging. During the packaging process, the chip experiences heating and cooling. Different expansion of MEMS structure, substrate and packaging leads to stress and structural deformation. [13]–[16].

There are three commonly used methods to reduce the stress. (1) Material selection: Materials whose CTE is similar to silicon are selected to complete the MEMS device packaging [18]–[20]. (2) Packaging method: The effect of die-bonding process on MEMS device performance was studied. Experimentally model used a distributed system-level nodal modeling in [21]. The research works in [22]–[24] focused on the attachment process such as the attachment area, attachment position, and four-dot die-attach process. (3) Stress isolation structures: Low stress packaging of micro machine accelerometer is reported in [9]. Stress relief structures formed around the periphery of the MEMS die was proposed in [9], [25]–[27]. A packaging-stress isolation structure designed on the handle layer of SOI is presented in [28], [29]. Besides, a two orthogonal stress-immunity structure [30] were designed to improve the temperature robustness of double-clamped MEMS sensors. However, the above method mentioned play a role of stress buffer to reduce the packaging stress, but the problem of CTE mismatch between the device structure and the substrate is not solved.

To suppress the thermal deformation caused by CTE mismatch, in addition to isolate packaging stress. A thermal deformation suppression chip (TDSC) for single center supported MEMS devices is presented. The chip is manufactured by the MEMS process and consists of an upper plate and a lower plate. The material of the upper plates is the same as that of the device substrate. So structure-substrate-TDSC is a sandwich like design. The position symmetry design of the materials can achieve the suppression of thermal deformation. A complete finite element model is established to verify the effect of TDSC. White-light interferometer is used to measure thermal deformation. The experiments show that the out-of-plane deformation can be eliminated by changing the anchor radius of TDSC. Temperature experiment is also performed to verify that the device deformation is insensitive to temperature variations due to the TDSC.

The paper is organized as follows: in section II, single center supported MEMS gyroscope is taken as an example to analyze the effect of CTE mismatch and the principle of TDSC. Section III describes the construction of the model to explore the relationship between anchor size of TDSC and thermal deformation. Section IV presents the experimental verification of the TDSC. Finally, the conclusion is presented in Section V.

II. DESIGN OF TDSC

A. ANALYSIS FOR THERMAL DEFORMATION OF SINGLE CENTER SUPPORTED MEMS GYROSCOPE

The MEMS resonant gyroscope has become one of the most important MEMS inertial sensors for detecting the angular velocity. Most MEMS resonant gyros work on the Coriolis principle. First, the electrostatic force is used to induce proof mass vibration. Then, under external angular velocity, the Coriolis force which is perpendicular to the driving direction and the direction of angular velocity is applied to the mass. The external angular velocity can be obtained by measuring the Coriolis force [3], [4].

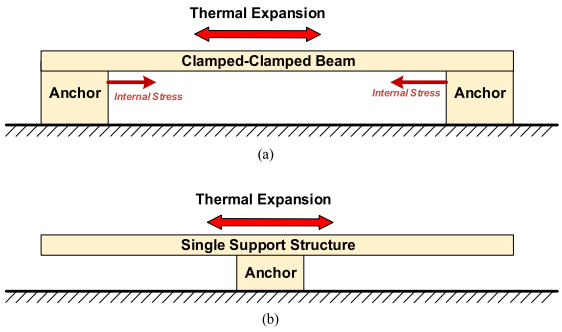

FIGURE 1. Schematic drawing of a clamped-clamped structure (a) and single support structure during thermal expansion (b).

As shown in Fig. 1(a), it is common to find clamped-clamped structures in the design of MEMS gyroscope [29]. However, due to the mismatch of the CTEs between the substrate and the device layer, expansion difference between structure and anchor will generate considerable stress. Aiming at the above problems, the single anchor design shown in Fig. 1(b) can effectively avoid internal stress. However, although the problem of internal stress is avoided by design, unexpected deformation shown in Fig.2 still exists, When

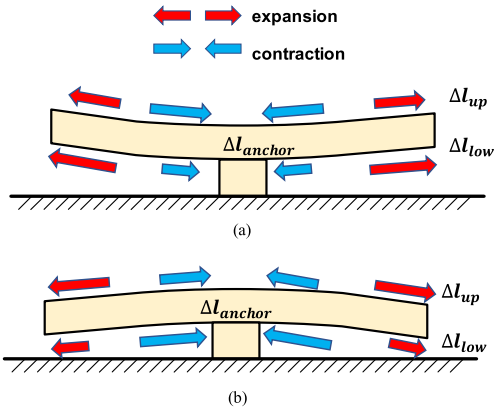

FIGURE 2. Thermal umbrella deformation of single anchor structure (a) and anti-umbrella-shaped deformation of single anchor structure (b).

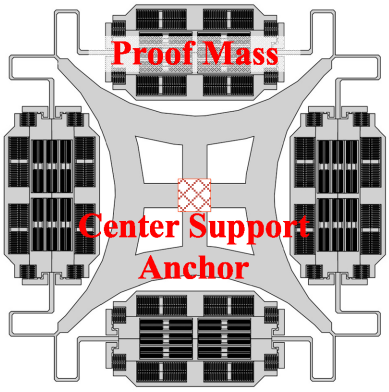

FIGURE 3. Structure of Center Support Quadruple Mass Gyroscope, with four proof masses connected through the N-shape-beams and the Y-shape-beams, supported by a single center support anchor.

$0 < \Delta l_{low} < \Delta l_{up}$ or $\Delta l_{low} < \Delta l_{up} < 0$, umbrella-shaped deformation shown in Fig. 2(a) occurs and it gets reversed when $0 < \Delta l_{up} < \Delta l_{low}$ or $\Delta l_{low} < \Delta l_{up} < 0$, as shown in Fig. 2(b). It should be noted that out-of-plane deformation occurs even for the gyroscope without any packaging, and deformation increases after packaging [17]. The thermal out-of-plane deformation leads to coupling signals and zero-bias changing, which is usually nonlinear with temperature and unpredictable. Thus, as for single center supported MEMS device, it is very important to reduce the deformation.

B. PRINCIPLE OF THERMAL DEFORMATION SUPPRESSION CHIP

As shown in Fig.3, the center supported quadruple mass gyroscope (CSQMG) is a typical MEMS device as described above [31], [32]. The CSQMG consists of four symmetrical proof masses, folding beams, and support frames. The movable structure is attached to the substrate by the center support anchor. To minimize the stress generated at the design level, clamped-clamped structure is avoided.

In this work, the CSQMG is fabricated based on the SOG process. Fig. 4(a) shows the process steps. A Pyrex substrate

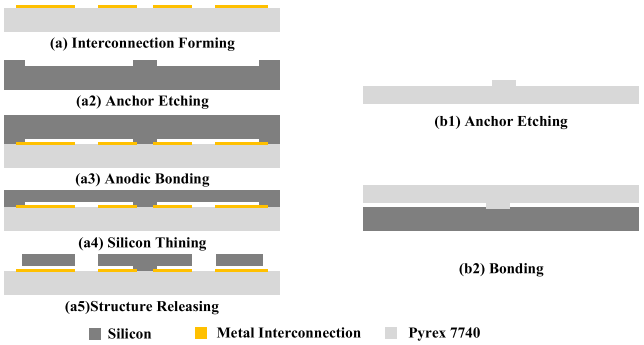

FIGURE 4. Process of CSQMG (a) and TDSC (b).

wafer and a silicon device wafer (100) were prepared for the gyro process. First, a 200nm thick Ti/Pt/Au layer was patterned using the liftoff process in the Pyrex wafer. Then, on one side of the silicon wafer, an anchor area with the height of 20μm was etched by DRIE. Afterwards, the device wafer and the substrate wafer were anodically bonded together at a temperature of 350°C with a DC voltage of approximately 500 V. Finally, the other side of the silicon wafer was thinned to 100 μm and released using the second DRIE step. As we know, the material of gyroscope structure is silicon but the substrate is Pyrex 7740 glass. Problem of CTE mismatch exists, so umbrella-shaped thermal deformation is the most important problem. Next, we will introduce TDSC to solve this problem.

For TDSC, we also adopt the single center anchor support design. It can be fabricated by the conventional MEMS process. The chip is obtained through two steps: 1) 50/200 nm Ti/Au was patterned as the mask. Then the Pyrex glass was put into the BOE solution(20:1), and the corrosion process lasted for 6.7 hours, forming a 20.5um anchor step. 2)Removing the metal mask, and the glass wafer is bonded to a silicon wafer (Fig. 4(b)). After wafer dicing, the chips are adhered use ABLEBOND JM7000 on ceramic shell to formed gyroscope with TDSC. Control the adhesive curing temperature within the range of 150 °C to 350 °C and curing under 300 °C for 15 minutes and cool to the room temperature. As shown in Fig. 5. The TDSC is located between the MEMS gyroscope substrate and the package shell. It is composed of upper and lower plates. The upper plate is attached to the substrate of gyro and is made of the same material as the MEMS device substrate. The upper and lower plates are bonded together by small central anchor.

The TDSC has two main functions. First, it works in isolating the packaging stress. Because of material matching, no packaging stress generates on the substrate of MEMS gyroscope. However, stress still occurs in areas where the CTEs are mismatched, such as (1) between the lower plate and ceramic shell and (2) between the upper plate and the lower plate. It is evident that all stress is transferred to the CSQMG structure only through the central anchor of TDSC. Accordingly, the single central anchor design isolates part of the packaging stress.

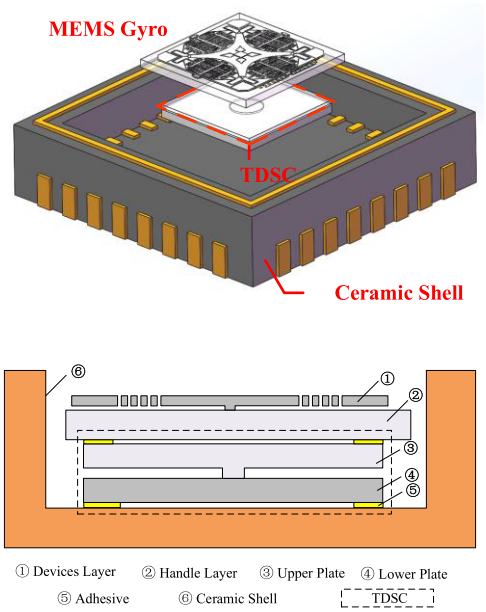

FIGURE 5. The schematic drawing of the MEMS gyro packaging with TDSC.

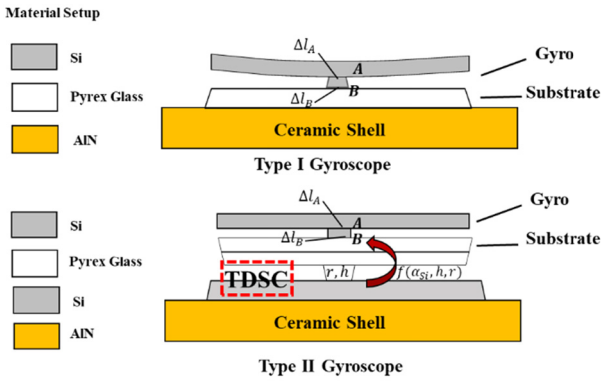

FIGURE 6. The schematic drawing of the TDSC for thermal deformation suppression by material matching.

The second function of the TDSC is suppressing the out-of-plane deformation of the CSQMG through symmetrical material setup. And the function is the purpose of TDSC. To explain the principle of symmetrical material setup further, we simplify the analysis using the follow assumptions:

1 Different component are considered as unions. The shape variables are the same at the contact surface.

2) The gyroscope deformation is determined by the thermal expansion of point A and B shown in Fig. 6. When $\Delta l_B > \Delta l_A$, umbrella-shaped deformation as Fig2.(a) occurs, and when $\Delta l_A > \Delta l_B$, anti-umbrella-shaped deformation occurs., and when $\Delta l_A = \Delta l_B$, no deformation is caused, which is the ideal state.

We defined two types of gyroscope: type I gyroscope was the packaged CSQMG without TDSC and type II gyroscope was without TDSC.

For the type I gyroscope, Δl_A is regarded as the free expansion of silicon anchor with radius l_A. The material setup

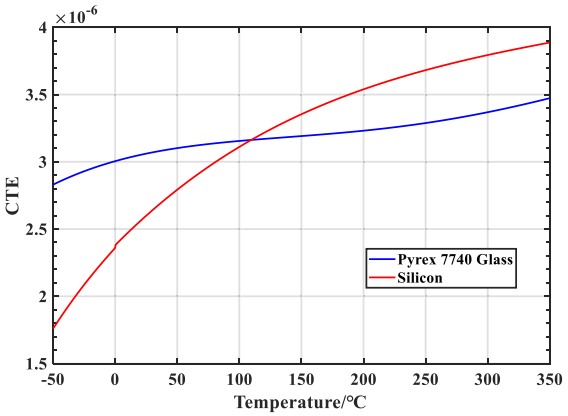

FIGURE 7. The thermal expansion coefficient of substrate (Pyrex 7740 glass) and device structure (Silicon 100).

is Si-Glass-AlN from the top to the bottom. According to the CTE data provided in [10], the CTE of Si and glass is shown in the Fig. 7. Pyrex7740 Glass CTE α_{glass} is larger than that of Si CTE α_{Si} before 109.5°, resulting in more thermal expansion on substrate glass. The thermal expansion difference between the substrate and the gyro structure forms the internal stress along the radial distribution on the material mismatch interface, which is proportional to the radius, resulting in the deformation of the gyro structure. Because the ceramic shell (AlN) CTE α_c is 3.3 ppm/°, so the deformation will be more obvious after being adhered to ceramic shell.

$$\begin{cases} \Delta l_A = L_A \int_{T_0}^{T_1} \alpha_{Si}(T)dT \\ L_A = L_B \\ |\Delta l_B| > |L_B \int_{T_0}^{T_1} \alpha_{Glass}(T)dT| > |L_A \int_{T_0}^{T_1} \alpha_{Si}(T)dT| > |\Delta l_A| \end{cases} \tag{2}$$

For the type II gyroscope, When TDSC is introduced, the material setup of type I gyroscope is "Si-Glass-Si-AlN", and the CTE order is "small-large-small-larger", which is like a sandwich structure. For the substrate, we hope that the CTE mismatch of the upper and lower surfaces can be adjusted to the same and opposite, resulting in no thermal deformation occurring on the surface of gyro. The thermal expansion of point A and B in the Fig. 6 can be expressed by equation (3):

$$\begin{cases} \Delta l_A = L_A \int_{T_0}^{T_1} \alpha_{Si}(T)dT \\ \Delta l_B = L_B \int_{T_0}^{T_1} \alpha_{Glass}(T)dT + f(a_{Si}, a_{Glass}, a_c, h, r) \end{cases} \tag{3}$$

We call the f a contribution function, which is TDSC's contribution to Δl_B.The contribution can be either negative or positive. In other word, the inequality, $|f| > 0$, is not always true. Changing the Δl_B to equal Δl_A is the purpose of contribution function, resulting in no thermal deformation on gyro structure. Obviously all that is connected to the glass is only the center support anchor of TDSC, and the CTE of silicon and shell is constant, so the dimension of the anchor is the key factor that determines the deformation

TABLE 1. Model dimensions.

Description	Dimensions(μm)
Gyro outline dimensions	8000×8000
TDSC outline dimensions	7000×7000
Upper plate thickness	480
Anchor height	20
Anchor radius	1000
Lower plate thickness	500
Ceramic radius	20000

state of gyroscope, so the function is related to the anchor parameter of TDSC when the overall size is determined. However, it is difficult to obtain the accurate value of the distribution force on the material mismatch interface and the deformation caused using mathematical method. In the next chapter, the finite element simulation is carried out simulation for studying.

III. FINITE ELEMENT SIMULATION AND VERIFICATION

A. FE MODELING

To study the modified function mentioned above and verify the effect on stress isolation, the finite element (FE) analysis model for the two types of gyroscope were built in COMSOL Multiphysics for comparison and verification. In the simulation, the upper plate material was made as silicon and the lower plate was Pyrex7740 glass. In the packaging process, the gyroscope chip was attached to the ceramic shell using an Ag adhesive at a temperature of 200°C; therefore, the structure was assumed to have no thermal expansion at 200°C. Additionally, the ceramic base bottom was constrained as the datum plane for calculating, which was required in the emulator. To reduce computation complexity, the models were simplified by replacing the irrelevant comb part with flat plate. Stationary simulation was carried out at 293.15K. The model dimension details are shown in Table 1.

B. CONTRIBUTION FUNCTION OF TDSC

According to Chapter II, both the packaging stress and out-of-plane deformation are caused by CTE mismatching. TDSC is a way to solve the problem through material symmetry setup. TDSC makes the equivalent CTE of the substrate the same as the structure, so as to achieve the purpose of restraining thermal deformation. All the parameters shown in Table 1 may determine the deformation state of gyroscope. However, considering the process steps, experimental verification cost and practicability, we choose the dimension of the TDSC anchor as the key factor. We expect to obtain the optimal dimensions for no deformation. Meanwhile, the packaging stability and process simplicity should be considered, which means that the anchor height should be small, and the area should be as large as possible. A cutting line a-b-c-d-e through the proof mass, frame, and center support anchor was created to describe the umbrella-shaped deformation of CSQMG (Fig. 8). The height difference between the center (point c)

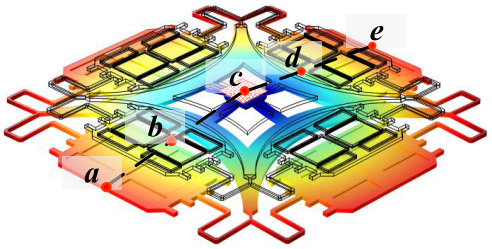

FIGURE 8. The umbrella-shape deformation magnified 200 times of CSQMG and cutting line in FEM.

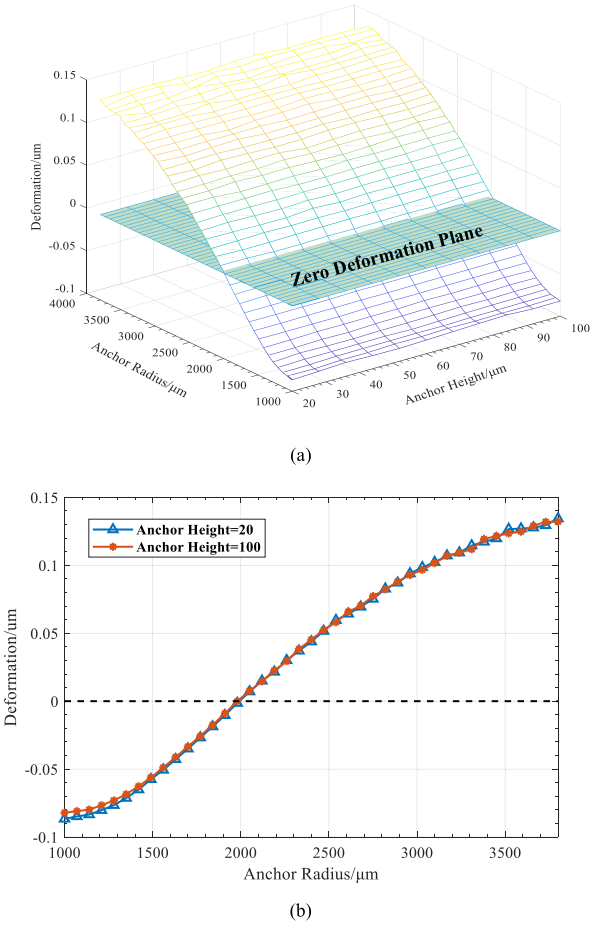

FIGURE 9. The relationship between anchor diameter of TDSC and the out of plane deformation (a); the relationship between anchor radius of TDSC and the out of plane deformation (b).

and the edge of the mass (point a or e) is taken as the observed thermal deformation.

The result of the diameter simulation is shown in Fig. 9(a). the z axis is the maximum warpage (the height difference between point a and point c in Fig.8). With the change in the size of the anchor, the out-of-plane deformation surface passes through the zero-deformation plane. We consider two curves with an anchor height of 20 and 100μm, respectively, and draw them in Fig. 9(b). The result shows that the out-of-plane deformation is independent of anchor height and is mainly affected by the radius of anchor.

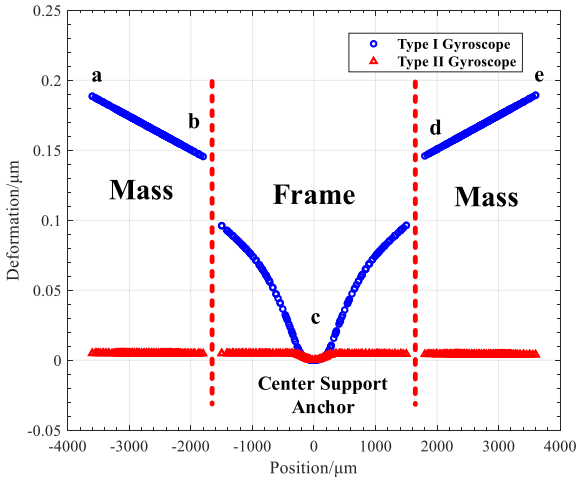

FIGURE 10. Out-of-Plane deformation of two types of gyroscope.

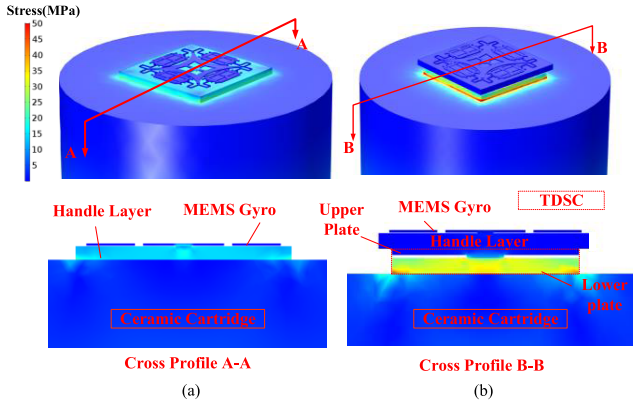

FIGURE 11. The simulation results of the stress distribution of Type I gyroscope (a) and Type II gyroscope (b) at 293.15K.

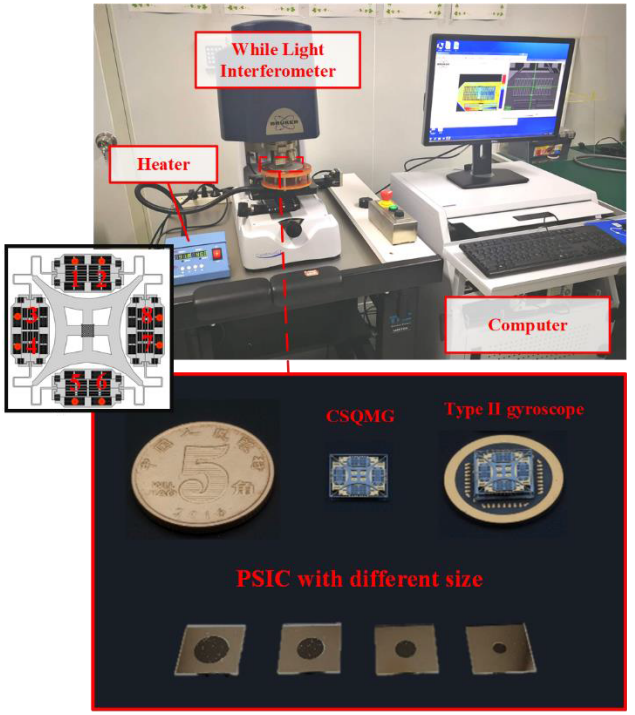

FIGURE 12. Photograph of the experimental platform, CSQMG and TDSC; TDSC is processed in anchor radius of 1000μm, 1400μm, 2000μm, and 2500μm. The middle figure is 8 measurement points position on the gyro.

TABLE 2. Average stress of two types of Gyroscope.

Stress (MPa)	TYPE I Gyroscope	Type II Gyroscope
Surface of substrate	29.4	0.76
Surface of Gyro	11.873	0.642

As the radius increased, the gyroscope gradually changed from reverse deformation to positive deformation, so zero-deformation can be achieved by changing the radius of anchor. To clearly demonstrate the zero-deformation of CSQMG, we chose a height and radius of 20 and 2120 μm, respectively, to simulate the out-of-plane deformation of two types of gyroscope. As shown in Fig. 10, the abscissa represents the position of the cutting line, where the coordinate of point C is 0. For the type I gyroscope, the maximum warpage is 0.1895μm. Owing to the TDSC, the out-of-plane deformation of type II gyroscope is almost completely suppressed, the maximum warpage is only 0.0049 um.

C. SIMULATION OF PACKAGING STRESS ISOLATION

As mentioned above, thermal deformation suppression and packaging stress isolation is two function of the TDSC. The transfer channel of the packaging stress follows the path: lower plate-central anchor-upper plate-gyroscope. It is evident that the central anchor is the only way to transfer the packaging stress. Stationary simulation was carried out to obtain the effect of TDSC on stress distribution at 25°. In simulation, the mismatch between the thermal expansion coefficients was the only source of stress. Ignoring the external stress effects, we set the ceramic thickness so large that no fixed stress will transfer to the gyroscope. Besides, the stress type is equivalent von Mises stress, which is an equivalent stress based on shear strain energy. It is defined:

$$\delta = \sqrt{\frac{(a_1 - a_2)^2 + (a_2 - a_3)^2 + (a_3 - a_1)^2}{2}} \tag{4}$$

where a_1, a_2, a_3 is the first, second and third principal stresses.

As shown in Fig.11, packaging stress occur in where the CTEs mismatch. The thermal stress of type I gyroscope is generated in the follow two places: 1) The bottom of gyro substrate and the ceramic shell; 2) The gyro anchor and substrate. On the substrate, it is obvious that the former account for a large stress. For type II gyroscope shown in Fig.11 (b), the stress is mainly concentrated between the ceramic shell and the lower plate, even though stress in the lower plate is larger than that in the substrate of type I gyroscope. Almost

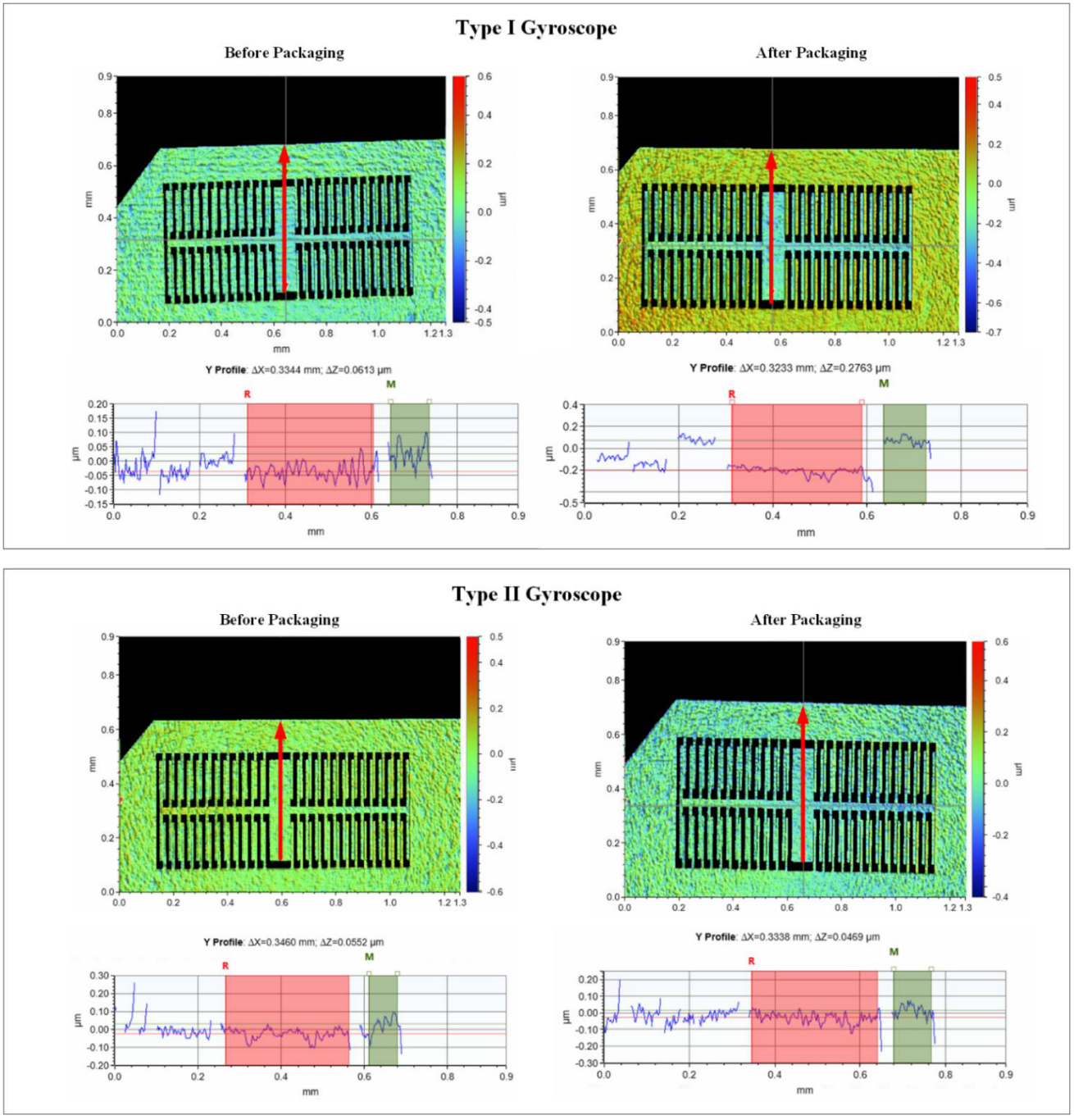

FIGURE 13. The thermal deformation of type I and type II gyroscopes before and after packaging.

all the packaging stress is concentrated in the area under the anchor of TDSC.

To accurately show the stress isolation effect, average stress of surface of substrate and surface of gyro is calculated for comparison. The result is shown in Table 2. The stresses in the surface of substrate of type I gyroscope and type II gyroscope are 29.4 and 0.76 MPa, respectively, and those in the surface of gyro are 11.873 and 0.642 MPa, respectively, so the TDSC also plays a role in packaging stress isolation.

IV. EXPERIMENTAL VERIFICATION

A. EXPERIMENT SETUP

In this work, the CSQMG and TDSC were fabricated and packaged into type I and II gyroscope. In the experiment, the while light interferometer, Bruker Contour GT-IM shown in Fig.12, was used to measure the out-of-plane deformation. The test temperature was controlled by a small heater. We chose the edge of the movable structure area as the observation window. The window includes the movable structure

TABLE 3. Measurement results of white light interferometer.

Test Number	Type I Gyroscope Deformation(μm)			Type II Gyroscope Deformation(μm)		
	Before Packaging	After Packaging	Deformation Variation	Before Packaging	After Packaging	Deformation Variation
1	0.0463	0.2423	0.196	0.0606	0.0477	-0.0129
2	0.0228	0.2123	0.1895	0.0365	0.0861	0.0496
3	0.0047	0.1561	0.1514	0.0098	0.102	0.0922
4	0.1138	0.2753	0.1615	0.0996	0.0809	-0.0187
5	0.0601	0.124	0.0639	0.0605	0.02385	-0.03665

and the static comb, the static comb is bonded to the substrate. Thus, we take the height difference between the movable structure and the static comb as the out-of-plane deformation of the gyro. To ensure the accuracy of test results, all four mass were measured for each gyro. Each mass contained two test points. The average measurement value of eight points (Fig.12) was taken as the deformation value of the gyro.

B. OUT-OF-PLANE DEFORMATION

Firstly, the relationship between the anchor radius (r) of TDSC and the out-of-plane deformation (Δz) was measured. As shown in Fig.9, the point of zero deformation is between 1500 and 2500μm. The fitted curve is approximately linear. Therefore, the radius of the experiment is set between 1000-2500μm. the simulation and experimental results are fitted linearly for simplify. TDSC with four different sizes was processed, as shown in Fig. 12. Then, these chips were packaged with CSQMG and tested under the same conditions. The results of experiment (Δz_1) and simulation (Δz_2) are shown in Fig. 14. The relationships are fitted as following.

$$\Delta z_1 = 1.731 \times 10^{-4} \cdot r - 0.3994 \quad (5)$$

$$\Delta z_2 = 9.732 \times 10^{-5} \cdot r - 0.2083 \quad (6)$$

The experimental results are in accordance with the simulation results. With the change of anchor radius, the deformation state turns from anti-umbrella shape to umbrella shape, and goes through no deformation state. For the radius of zero-deformation, experiment and simulation are 2307.3 and 2140.3μm, respectively, with a 7.8% relative error. Because simplified gyroscope model is used in the simulation and the influence of adhesives is neglected. The mismatch between the values of thermal expansion is the only source of out-of-plane deformation, and we ignore the residual stress in chip processing, which is difficult to estimate.

Then, we choose the TDSC with 2500um to verify the effect of TDSC on suppressing the out-of-plane deformation. Firstly, 10 gyroscopes without packaging were measured by the while light interferometer As shown in Table 3, the initial thermal out-of-plane deformation is distributed between 0.0047μm and 0.1138μm. The initial deformation is caused by residual stress in the wafer process, like anodic bonding. Then, the 10 gyroscopes are packaged into 5 type I and 5 type II gyroscopes, and measured again. Figs.13(a) and (b) show the measured result of type I and type II gyroscopes before and after packaging, respectively, which is just one of all measurement points. The average measurement value of eight points data is listed in Table 3.

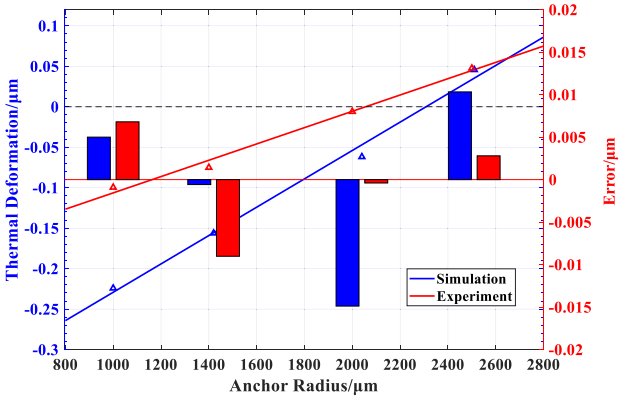

FIGURE 14. Comparison between simulation (blue line) and experiment (red line) on the relationship between anchor radius and out-of-plane deformation.

To clearly describe the suppression effect of TDSC on thermal deformation, the thermal deformation variation after packaging of the two types of gyros are shown in figure 15. The blue bar is the type I gyroscope, and the thermal out-of-plane deformation after packaging is obviously increased. For the type II gyroscope (red bar), which is packaged with TDSC, the thermal deformation variation is smaller than that of type I gyroscope, or even smaller than 0, which means that thermal deformation of type II gyroscope is smaller than gyro without any packaging. Actually, the packaging stress is never smaller than that without packaging, the TDSC suppresses the deformation directly by material symmetry setting.

C. TEMPERATURE EXPERIMENT

Temperature is the most significant factor that affects the output of a MEMS gyroscope. Temperature also causes stress variation. To verify the improvements in the temperature performance of gyroscope with TDSC, white light interference experiment under variable temperature conditions was conducted. In the experiment, two types of gyroscopes were heated from 20 °C to 140 °C and measured. We set every 20 °C as a measuring point and keep each point for 2 hours. As shown in Fig. 16, the deformation decreases with the increase in temperature because the operating temperature of packaging is usually higher ($T < T_0$ in equation (1)).

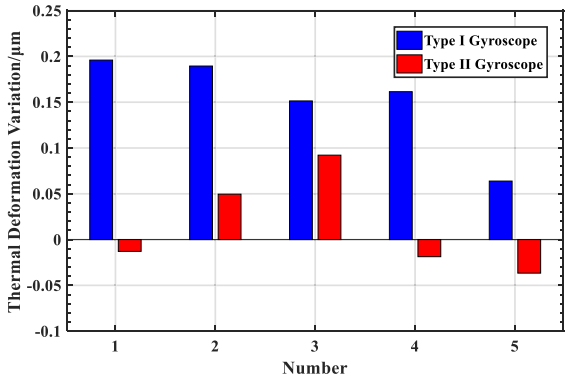

FIGURE 15. Thermal deformation Variation after packaging of the two types of gyroscope.

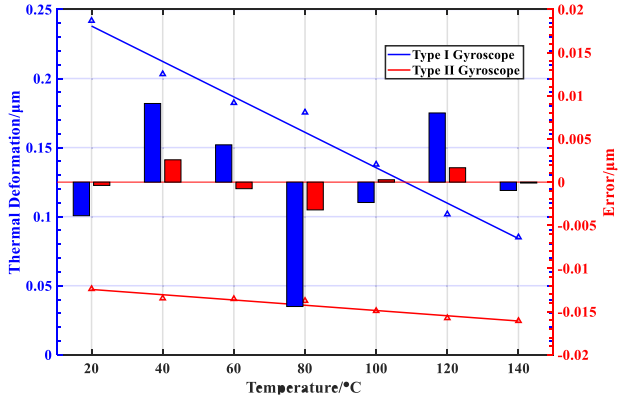

FIGURE 16. Temperature structure deformation comparison of two types of gyroscopes.

For type I gyroscope, the deformation changes from 0.2423 to 0.085μm. The deformation change in the whole temperature experiment is 0.1573μm, and that of type II gyroscope is 0.0257μm, which is only 0.15 times of that of type I gyroscope. It is obvious that type II gyroscope is more insensitive to temperature change, which means that TDSC can not only reduce the umbrella-shaped deformation but also enhance the robustness of the gyroscope in variable temperature environment.

V. CONCLUSION AND DISCUSSION

From the above experimental results, TDSC can restrain the out-of-plane deformation of single anchor device structure, which is helpful to improve the performance and thermal environment adaptability of MEMS devices. In addition, the following further improvements can be applied to TDSC:

1) The TDSC is suitable for MEMS devices with various substrates. The material of the upper and lower plate should be the same as that of the MEMS device and substrate. The TDSC can be manufactured simultaneously with MEMS devices. First, the substrate of the device wafer must be etched to create the anchor. Then, the device wafer after anchor etching is bonded to the lower plate wafer. Finally, the MEMS devices with TDSC can be obtained by scribing. However, this method adds the processing steps of MEMS devices and the substrate layer may have the problem of secondary bonding. In comparison to the TDSC processed separately, the effect of stress isolation will be weakened due to the decrease in the thickness of the upper plate.
2) The lower plate of TDSC can also be etched to form the stress isolation pattern, which can further help to obtain a better stress isolation effect. The effect of the overall size of TDSC on the stress isolation effect can be neglected. The upper plate area is large enough to ensure the operability of subsequent packaging. Therefore, once a TDSC is processed, it can be applied to other MEMS devices with the same substrate.

In summary, to solve the problem of thermal deformation caused by CTEs mismatch, a thermal deformation suppression chip (TDSC) based on MEMS process is proposed. The principle of TDSC is building a sandwich like material symmetrical structure, to achieve the CTEs' mismatch symmetrical between the two surface of device substrate. Besides, Single anchor support design is adopted, and the CTE mismatch can be adjusted by the size of single anchor. This study focuses on center supported quadruple mass gyroscope to establish the mathematical and finite element models of TDSC, providing the influence of TDSC on packaging stress distribution and out-of-plane deformation of MEMS gyroscope. In addition, the white light interferometer experiment was carried out. Simulation and experiment show that the optimal effect of thermal deformation suppression can be achieved by changing the anchor radius, and out-of-plane deformation was significantly reduced in the gyroscopes with TDSC, which is better than that of the gyroscope without packaging. Simultaneously, we also demonstrate the ability of TDSC to improve the thermal environment adaptability of the MEMS gyroscope. Furthermore, chip-level format makes TDSC suitable for other MEMS devices with single center anchor.

REFERENCES

[1] N. Yazdi, F. Ayazi, and K. Najafi, "Micromachined inertial sensors," *Proc. IEEE*, vol. 86, no. 8, pp. 1640–1659, Aug. 1998.
[2] M. W. Judy, "Evolution of integrated inertial MEMS technology," in *Proc. Solid-State Sens., Actuator, Microsyst. Workshop*, Hilton Head Island, SC, USA, Jun. 2004, pp. 27–32.
[3] A. Sharma, M. F. Zaman, M. Zucher, and F. Ayazi, "A 0.1°/HR bias drift electronically matched tuning fork microgyroscope," in *Proc. IEEE 21st Int. Conf. Micro Electro Mech. Syst.*, Jan. 2008, pp. 6–9.
[4] A. A. Trusov, G. Atikyan, D. M. Rozelle, A. D. Meyer, S. A. Zotov, B. R. Simon, and A. M. Shkel, "Flat is not dead: Current and future performance of Si-MEMS quad mass gyro (QMG) system," in *Proc. IEEE/ION Position, Location Navigat. Symp. (PLANS)*, May 2014, pp. 252–258.
[5] X. Song and S. Liu, "A performance prediction model for a piezoresistive transducer pressure sensor," in *Proc. 5th Int. Conf. Electron. Packag. Technol. (ICEPT)*, 2003, pp. 30–35.
[6] T. Naito, N. Konno, T. Tokunaga, and T. Itoh, "Doping characteristics of polycrystalline silicon deposited by chemical transport at atmospheric pressure and its application to MEMS sensor," *IEEE Sensors J.*, vol. 13, no. 8, pp. 2899–2905, Aug. 2013.
[7] A. L. Roy, H. Sarkar, and A. Dutta, "A high precision SOI MEMS–CMOS ±4g piezoresistive accelerometer," *Sens. Actuators A, Phys.*, vol. 210, pp. 77–85, Apr. 2014.

[8] G. Dai, M. Li, X. He, L. Du, B. Shao, and W. Su, "Thermal drift analysis using a multiphysics model of bulk silicon MEMS capacitive accelerometer," *Sens. Actuators A, Phys.*, vol. 172, no. 2, pp. 369–378, Dec. 2011.
[9] G. Li and A. A. Tseng, "Low stress packaging of a micromachined accelerometer," *IEEE Trans. Electron. Packag. Manuf.*, vol. 24, no. 1, pp. 18–25, Jan. 2001.
[10] J.-W. Joo and S.-H. Choa, "Deformation behavior of MEMS gyroscope sensor package subjected to temperature change," *IEEE Trans. Compon. Packag. Technol.*, vol. 30, no. 2, pp. 346–354, Jun. 2007.
[11] M. Gonzalez, A. Jourdain, B. Vandevelde, and H. A. C. Tilmans, "Effect of thermomechanical stress on resonant frequency shift of a silicon MEMS resonator," in *Proc. EuroSimE Int. Conf. Thermal, Mech. Multi-Phys. Simul. Exp. Microelectron. Micro-Syst.*, Apr. 2008.
[12] E. Tatar, T. Mukherjee, and G. K. Fedder, "On-chip characterization of stress effects on gyroscope zero rate output and scale factor," in *Proc. 28th IEEE Int. Conf. Micro Electro Mech. Syst. (MEMS)*, Jan. 2015, pp. 813–816.
[13] H. Johari-Galle and M. W. Judy, "MEMS device with stress relief structures," U.S. Patent 9 676 614, Jun. 13, 2017.
[14] K. V. Shcheglov, N. F. Maggipinto, D. Smukowski, and C. Sun, "MEMS stress isolation and stabilization system," U.S. Patent 10 278 281, Apr. 30, 2019.
[15] C.-L. Lu and M.-K. Yeh, "Thermal stress analysis for a CMOS-MEMS microphone with various metallization and materials," *Microelectron. Eng.*, vol. 213, pp. 47–54, May 2019.
[16] P. Peng, W. Zhou, H. Yu, B. Peng, H. Qu, and X. He, "Investigation of the thermal drift of MEMS capacitive accelerometers induced by the overflow of die attachment adhesive," *IEEE Trans. Compon., Packag., Manuf. Technol.*, vol. 6, no. 5, pp. 822–830, May 2016.
[17] A. Gerlach, D. Maas, D. Seidel, H. Bartuch, S. Schundau, and K. Kaschlik, "Low-temperature anodic bonding of silicon to silicon wafers by means of intermediate glass layers," *Microsyst. Technol.*, vol. 5, no. 3, pp. 144–149, Feb. 1999.
[18] T. Rogers and J. Kowal, "Selection of glass, anodic bonding conditions and material compatibility for silicon-glass capacitive sensors," *Sens. Actuators A, Phys.*, vol. 46, nos. 1–3, pp. 113–120, Jan. 1995.
[19] S. S. Walwadkar and J. Cho, "Evaluation of die stress in MEMS packaging: Experimental and theoretical approaches," *IEEE Trans. Compon. Packag. Technol.*, vol. 29, no. 4, pp. 735–742, Dec. 2006.
[20] H. K. Kopola, J. Lenkkeri, and K. Kautio, "MEMS sensor packaging using LTCC substrate technology," *Proc SPIE*, vol. 4592, pp. 148–158, Nov. 2001.
[21] J. Song, Q.-A. Huang, M. Li, and J.-Y. Tang, "Effect of die-bonding process on MEMS device performance: System-level modeling and experimental verification," *J. Microelectromech. Syst.*, vol. 18, no. 2, pp. 274–286, Apr. 2009.
[22] T. Königer, "New die attach adhesives enable low-stress MEMS packaging," in *Proc. 36th Int. Electron. Manuf. Technol. Conf.*, Nov. 2014, pp. 1–5.
[23] B. R. Simon, G. Sharma, S. A. Zotov, A. A. Trusov, and A. M. Shkel, "Intrinsic stress of eutectic Au/Sn die attachment and effect on mode-matched MEMS gyroscopes," in *Proc. Int. Symp. Inertial Sensors Syst. (ISISS)*, Feb. 2014, pp. 1–4.
[24] S. Schroder, F. Niklaus, A. Nafari, E. R. Westby, A. C. Fischer, G. Stemme, and S. Haasl, "Stress-minimized packaging of inertial sensors by double-sided bond wire attachment," *J. Microelectromech. Syst.*, vol. 24, no. 4, pp. 781–789, Aug. 2015.
[25] H. Johari-Galle and M. W. Judy, "MEMS device with stress relief structures," U.S. Patent 2014 0217 521 A1, Aug. 7, 2014.
[26] H.-S. Hsieh, H.-C. Chang, C.-F. Hu, C.-L. Cheng, and W. Fang, "A novel stress isolation guard-ring design for the improvement of a three-axis piezoresistive accelerometer," *J. Micromech. Microeng.*, vol. 21, no. 10, Sep. 2011, Art. no. 105006.
[27] Z. Chen, M. Guo, R. Zhang, B. Zhou, and Q. Wei, "Measurement and isolation of thermal stress in silicon-on-glass MEMS structures," *Sensors*, vol. 18, no. 8, p. 2603, Aug. 2018.
[28] Y. Hao, W. Yuan, J. Xie, and H. Chang, "A novel packaging stress isolation structure for SOI based MEMS gyroscopes," in *Proc. IEEE SENSORS*, Oct. 2016, pp. 1–3.
[29] Y. Hao, W. Yuan, J. Xie, Q. Shen, and H. Chang, "Design and verification of a structure for isolating packaging stress in SOI MEMS devices," *IEEE Sensors J.*, vol. 17, no. 5, pp. 1246–1254, Mar. 2017.
[30] X. Wang, D. Xiao, Z. Hou, Q. Li, Z. Chen, and X. Wu, "Temperature robustness design for double-clamped MEMS sensors based on two orthogonal stress-immunity structure," in *Proc. IEEE SENSORS*, Nov. 2015, pp. 1–4.
[31] T. Zhang, B. Zhou, M. Song, Z. Lin, S. Jin, and R. Zhang, "Structural parameter identification of the center support quadruple mass gyro," *IEEE Sensors J.*, vol. 17, no. 12, pp. 3765–3775, Jun. 2017.
[32] T. Zhang, B. Zhou, P. Yin, Z. Chen, and R. Zhang, "Optimal design of a center support quadruple mass gyroscope (CSQMG)," *Sensors*, vol. 16, no. 5, p. 613, Apr. 2016.

BOWEN XING was born in Henan, China, in 1995. He received the B.S. degree in precision instruments from Tsinghua University, Beijing, China, in 2017, where he is currently pursuing the Ph.D. degree with the State Key Laboratory of Precision Measuring Technology and Instruments. His main research interest is MEME gyroscope.

BIN ZHOU received the B.S. and Ph.D. degrees in precision instruments from Tsinghua University, Beijing, China, in 1998 and 2004, respectively. From 2004 to 2010, he was an Assistant Professor of MEMS inertial sensor with the Department of Precision Instruments, Tsinghua University, where he has been an Associate Professor, since 2010. His research interests are in the fields of MEMS inertial sensors, digital signal process, and sensor ASIC design.

XINXI ZHANG received the Ph.D. degree from the Department of Precision Instrument, Tsinghua University, Beijing, China, in 2016. He is currently an Assistant Professor with the Weapon and Control Department, Army Academy of Armored Forces. His current research interests include inertia measurement and inertia navigation.

WENMING ZHANG received the B.S. degree from the Xi'an University of Post and Telecommunications, in 2007, and the M.S. degree in control science and engineering from the National University of Defense Technology, Changsha, China, in 2009. He is currently pursuing the Ph.D. degree in instrumentation science and technology with Tsinghua University, Beijing, China. His main research interests include design of MEMS gyroscopes and MEMS manufacturing processes.

BO HOU was born in Sichuan, China, in 1991. He received the B.Sc. degree from Chongqing University, in 2015. He is currently pursuing the Ph.D. degree with the State Key Laboratory of Precision Measuring Technology and Instruments, Tsinghua University, Beijing, China. His main research interests are MEMS inertial sensor and angular sensor.

QI WEI received the Ph.D. degree from Tsinghua University, Beijing, China, in 2010. He is currently an Assistant Professor with the Department of Precision Instruments, Tsinghua University. His research interests are MEMS inertial sensors, ASIC design, and high performance data converters.

TIAN ZHANG received the B.S. degree in precision instruments from Tsinghua University, Beijing, China, in 2018, and the Ph.D. degree in instrumentation science and technology from Tsinghua University. His current research interests include structure design of MEMS gyroscopes and new MEMS manufacturing processes.

RONG ZHANG received the B.S. degree in mechanical design and manufacturing and the M.S. and Ph.D. degrees in precision instruments from Tsinghua University, Beijing, China, in 1992, 1994, and 2007, respectively. In 1994, he joined the Faculty of Tsinghua University, where he became a Professor with the Department of Precision Instrument. His professional interests include precision motion control systems, MEMS inertial sensors, and integrated navigation systems.